Phonon structure in I-V characteristic of MgB_2 point-contacts

I. K. Yanson[1,2*], V. V. Fisun[1], N. L. Bobrov[1], and Yu. G. Naidyuk[1]
[1] *B.Verkin Institute for Low Temperature Physics and Engineering, National Academy of Sciences of Ukraine, 47 Lenin Ave., 61103, Kharkiv, Ukraine and*
[2] *Forschungzentrum Karlsruhe GmbH, Technik und Umwelt, Postfach 3640, D-76021, Karlsruhe, Germany*

W. N. Kang, Eun-Mi Choi, Hyun-Jung Kim and Sung-Ik Lee
National Creative Research Initiative Center for Superconductivity, Department of Physics, Pohang University of Science and Technology, Pohang 790-784, South Korea
(Dated: February 1, 2008)

The search of the phonon structure at the above-gap energies was carried out for $d^2V/dI^2(V)$ spectra of MgB_2 point contacts with a normal metal. The two-band model is assumed not only for the gap structure in $dV/dI(V)$-characteristics, but also for phonons in $d^2V/dI^2(V)$ point-contact spectra, with up to the maximum lattice vibration energy. Since the current is carried mostly by charges of 3D-band, whereas the strong electron-phonon interaction occurs in 2D-band, we observe the phonon peculiarities due to "proximity" effect in k-space, which depends both on the contact orientation with respect to the crystal axes and the variation of interband coupling through the elastic scattering.

PACS numbers: 74.25Fy, 74.80.Fp, 73.40.Jn

Introduction.

The superconducting properties of the newly discovered *s-p* compound MgB_2 [1] have been attracting recently much attention of the superconductive community. The relatively high $T_c \simeq 39$ K, the absence of magnetic order and strongly correlated charge carriers, on the one hand, and the strong links between grains for large enough critical currents and magnetic fields, on the other hand, make it very promising for complete understanding of the superconducting mechanism and its successful applications at moderate temperatures [2].

Unfortunately, the simplicity of this compound does not go too far for immediate understanding of all details of its superconducting mechanism. From the theoretical point of view, this compound appears to be a rare example of several (at least two) disconnected bands of the Fermi surface (FS) with quite different dynamical properties [3, 4, 5]. The theory predicts that one of those is two-dimensional (2D), with strong electron-phonon interaction (EPI), while the other is 3D with weak EPI and even larger density of states at the Fermi energy [4, 5, 6]. The interband scattering between these two parts is weak [5], and they behave like an "intrinsic proximity effect" [7]. The superconducting and normal parts are not separated spatially, like in the McMillan model [8, 9] of SN sandwiches, but are weakly connected in k-space through the interband scattering. In connection with this behavior, one has to recall earlier works of two-band superconductivity [10, 11, 12]. But there is an important difference between the predictions of those old papers and what is observed in Ref.[7] and some other point-contact and tunneling works (see, for example, Refs.[13, 14]). Since the 2D and 3D parts of Fermi surface are very anisotropic, the tunneling and point-contact current depends strongly on the orientation with respect to the crystal axes, and for c-orientation the contribution of the 3D band prevails [15]. Superconducting energy gap values, corresponding to these two bands, differ very much (up to the factor of 3 [15, 16]), and turn to zero at the same critical temperature $\sim 38-40$ K. Moreover, if the separate energy gaps converge to a single averaged gap, the critical temperature remains almost the same. Possible explanation of this behavior [15] is that the charges of the 3D band play much greater role in the PC current, due to the higher Fermi velocity and larger plasma frequency. By analogy, the situation looks as if one measures superconducting energy gap only from the "normal' side of the McMillan sandwiches in coordinate space. T_c does not decrease noticeably with increasing elastic scattering, since the latter is not strong enough.

Luckily, in MgB_2 no other bosonic excitation, except phonons, is anticipated [5, 16, 17]. Thus, the only mechanism of the formation of Cooper pairs is EPI, although when a new superconductor with relatively high T_c is discovered, other mechanisms are always proposed.

In spite of great variety of spectroscopic measurements, which convincingly show the existence of two different superconducting energy gaps belonging to the above mentioned two parts of FS (see, for example, Refs.[13, 18], and more recent papers [7, 14]), there are only a few reports of direct experimental proof for phonon structure in the point-contact characteristic [19] or tunneling [20].

In this paper we present the first attempt to identify the structure of MgB_2 point-contact (PC) spectra at energies up to the maximum phonon frequency. We show that the observed peculiarities are unequivocally caused

*Corresponding author, e-mail: yanson@ilt.kharkov.ua

by phonons, and their appearance correlates with the observed superconducting energy gap for a given point contact. In our opinion, this is due to the strong anisotropy of multi-band electron and phonon spectra, and to the influence of the elastic scattering, which determines both the intraband and interband EPI coupling in this compound. The random deviation of the contact axis from the predominantly c-direction plays a crucial role.

Specific of experiment

The samples are *c*-axis oriented films of MgB_2, whose characteristics are described in Refs.[18, 21]. The contacts are made by direct touch of MgB_2 with a sharpened normal metal electrode (Cu or Ag). The axis of the contact nominally coincides with the *c*-axis of the film, and thus, determines the main direction of the current. The orientation selectivity in the point-contact spectroscopy is low (lower, than in plane tunnel junction, where it goes exponentially), and is within a solid angle of roughly a few tens of degrees. Moreover, since not every touch produces the desired appearance of the energy-gap I-V characteristic, we moved the electrodes relative to each other in order to penetrate through the accidentally damaged surface layer. This operation changes the contribution of the perpendicular *ab*-direction and produces additional defects in the contact region and, thus, shortens further the small electron mean free path. In a few experiments we tried to make a contact with a broken side-face of the film, in order to increase the occurrence of *ab*-direction for the current.

Thus, our "input" characteristic is the shape of superconducting energy-gap structure, which is described elsewhere [18, 19]. The main goal is to investigate the first and second derivatives of the I-V characteristic at large biases, providing the contact survives the long-term measurements.

The attractive feature of PC spectroscopy is that the measured second derivative for the normal state turns out to be directly proportional to EPI function $\alpha^2(\omega)\,F(\omega)$ [22, 24]

$$\frac{\mathrm{d}^2V}{\mathrm{d}I^2} \propto \frac{\mathrm{d}(\ln R)}{\mathrm{d}V} = \frac{8\,ed}{3\,\hbar v_{\mathrm{F}}}\alpha^2(\omega)\,F(\omega) \qquad (1)$$

where α, roughly speaking, describes the strength of the electron interaction with one or another phonon branch for electron transport through the contact with diameter d, $F(\omega)$ stands for the phonon density of states. In PC spectra the EPI spectral function is modified by the transport factor, which increases strongly the backscattering processes.

However, in the superconducting state the above-gap singularity at phonon frequencies can be caused by several mechanisms [24, 25]. The features, which are strongly shifted along the voltage scale upon increasing the temperature and field, should be disregarded, as due to the nonequilibrium superconducting phenomena [24, 25]. Only those, whose positions do not depend on T, H, except the small shifts of the order of superconducting energy gaps (2÷7 meV), are considered.

The temperature is varied from 1.5 K up to $T \geq T_c$ with the magnetic field up to 4.5 T applied along the *ab*-plane. At low temperatures this field is not enough to destroy superconductivity. In order to observe the inelastic point-contact spectrum in the normal state, we raise both the temperature and the field.

The magnetic field does not influence the inelastic PC spectrum (1), because of the short mean free path. But it can strongly suppress superconductivity in the weakly superconducting 3D band, and destroy the exchange of the Cooper pairs from the strongly superconducting 2D-band. Since the current flows mostly from the 3D-band, the phonon structure appears indirectly, its intensity being strongly influenced by the field. Only small admixture of the direct 2D-band contributes to EPI, due to random inclusion of the *ab*-direction in the current.

Results and Discussion.

In Fig.1a the $dV/dI(V)$ and $V_2\,(eV) \propto d^2V/dI^2\,(eV)$ characteristics are shown in the superconducting state at zero field. In the energy-gap region the two gaps are clearly seen with $\Delta_1 = 2.4$ and $\Delta_2 = 5.7$ meV. Further on, we simply denote by Δ the position of dV/dI minimum. For many junctions we determine the superconducting energy gap by the BTK-fitting procedure [18]. For PC with not too large Γ-parameter, introduced by Dynes, this value does not differ too much from the true energy gap. The first derivative at above-gap energies is slightly asymmetric and nearly parabolic, which leads to an approximately linear background in $d^2V/dI^2(V)$. This background is subtracted from the raw $V_2(V)$-dependence, and the result is shown by curve 2 (panel a). The latter curve displays an antisymmetric structure, whose amplitude is about a fraction of percent in differential resistance. In the panel (b), this structure is compared with the phonon density of states (PDOS) [26]. Good correspondence is seen between the positions of PDOS peaks and maxima in $d^2V/dI^2(V)$.

The reproducibility of this PC spectra for different contacts can be seen in Fig.2a,b, where the raw data for three different junctions are shown. Here, the contact resistance varies from 43 to 111 Ω with gap minima at $\Delta = 2.1$, 2.6, and 4.86 meV, respectively. All the second derivative spectra (b) correlate with PDOS. The slight variation is probably due to the anisotropy and different scattering rates in the contacts. Compared with the theoretical EPI function (see, for example, Ref. [6, 17]), the peak at eV=60÷70 meV of E_{2g} boron mode is not too much higher in intensity, in accord with observation of Ref.[19].

According to our classifications of the energy gap structure [18], it is due to the random orientation of the contact axis and scattering of charge carriers between two band of Fermi surface, having gaps Δ_1 and Δ_2 mixed.

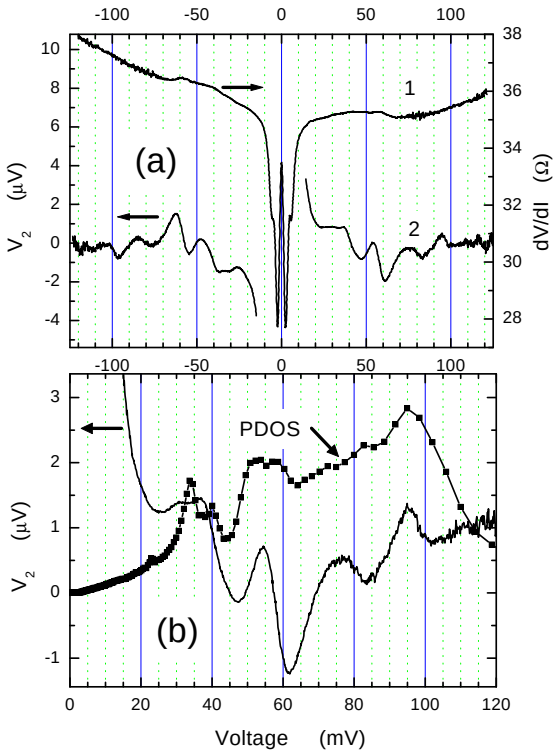

FIG. 1: a) **Curve 1**: Differential resistance $R = dV/dI(V)$ for MgB_2-Ag point contact. The structure at bias ¡10 mV shows two superconducting gaps corresponding to two different parts of the Fermi surface. The junction is made with the broken side-face of the film. **Curve 2**: The point-contact spectrum $V_2 \propto d^2V/dI^2$ of the same junction (V_2 is the second harmonic voltage with modulation voltage $V_1 = 2.52$ mV). $d(\ln R)/dV = 2\sqrt{2}V_2/V_1^2$, where $R = dV/dI(V)$. The linear background is subtracted from the raw data.
$T = 4.2$ K, $H = 0$, $R_0 = 35\ \Omega$.
b) The point-contact spectrum averaged between plus and minus V-polarity (the same, as in panel a), compared to the experimental phonon density of states of MgB_2 taken from Ref.[26]. The ordinate axis for PDOS is given in arbitrary units.

With an increase of interband scattering the magnitude of Δ_1 (Δ_2) moves to the higher (lower) value, respectively. For dirty contacts, where the admixture of the 2D-band is essential, only one maximum remains with a broad distribution around $\simeq 3.5$ meV [18], while T_c remains almost the same. In this case l is smaller than d (where l and d are the electron mean free path and the size of the contact, respectively), and the inelastic backscattering contribution to the phonon structure, proportional to l/d [23], is small. Therefore, in the superconducting state, the observed phonon structure presents mainly the elastic contribution to the excess current [24]. The elastic term is proportional to the energy dependent part of the excess current $I_{exc}(eV)$, similar to the phonon structure in the quasiparticle DOS for tunneling spectroscopy [24, 25]:

$$\frac{dI_{exc}}{dV}(eV) = \frac{1}{R_0}\left|\frac{\Delta_{in}(eV)}{eV + \sqrt{(eV)^2 - \Delta_{in}^2(eV)}}\right|^2, \qquad (2)$$

where $\Delta_{in}(eV)$ is the gap parameter in the 3D band, induced by 2D-band EPI. As seen in Fig.2, if the Δ value increases (panel a, curves 1-3), then the intensity of the phonon structure in the units of $d(\ln R)/dV = 2\sqrt{2}V_2/V_1^2$ increases too (panel b). That is because the modulation voltage V_1 decreases, whereas the amplitudes in $V_2(eV)$-units remain approximately the same. Note, that for curve 1 in Fig.2a one has to take the lower gap Δ_1, because the current is mainly determined by 3D-band, as mentioned above.

In Fig.3, the normal state spectrum is displayed together with the differential resistances in the superconducting state, showing the energy gap structure. In spite of a 10 times increase of the temperature smearing ($\simeq 20$ meV at 41 K instead of 2 meV at 4.2 K), the residual phonon structure is still visible in Fig.3b. The smeared phonon features are superimposed on the rising linear background. For curve 2, we see an increase in scattering at $\simeq 35$ meV, where the acoustic phonon peak occurs, and the saturation at $\simeq$100 meV, where the phonon spectrum ends. In the normal state, only those nonlinearities remain, which are due to the inelastic processes [22]. We stress that judging from the superconducting gap value ($\simeq 3.69$ meV for curve 2 in panel a) the essential contribution is expected from the $\Delta_2(E)$ of 2D-band for normal-state spectrum No.2. This spectrum should contrast with curve 6 in Fig.4 (see below), where the direct contribution from the 2D-band is small, due to lower value of Δ. Thus, the backscattering processes from the 3D-band are mostly essential here. The same is true for curve 6 in Fig.4, where the phonon features are not seen at high energies. The shape of spectrum 1 in Fig.3b presents the behavior intermediate between these two extremes, although its energy gap is approximately equal to curve 6 in Fig.4. Beside the well seen phonon spectral features in the range $30 \div 100$ meV, it possesses a low energy bump at about 20 meV.

Note, that the modulation voltages for spectra 1,2 in Figs.3b and 4 are the same. That means that they have the same second derivative scales, and the intensity of the second derivative is greater for curve 2 in Fig.3b, than those of curve 1 in Fig.3b and curve 6 in Fig.4.

The increasing second derivative of the I-V characteristic in the normal state is due to excess generation of nonequilibrium phonons at the contact. The PC spectra with phonon features in the normal state at T$\geq$ T$_c$, like those shown in Fig.3b, usually exhibit the nonequilibrium

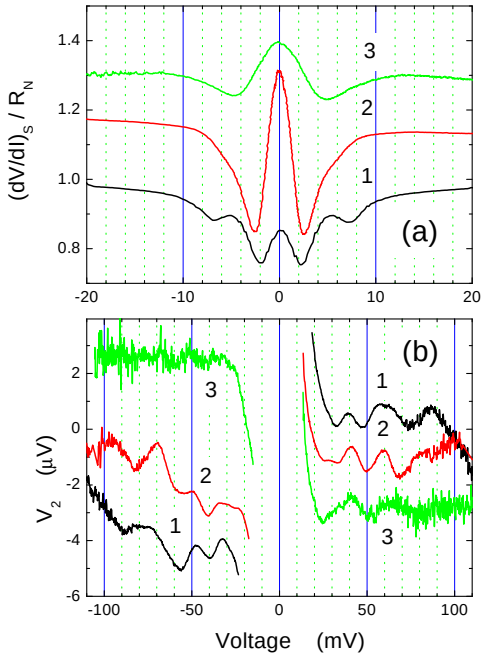

FIG. 2: (a) Differential resistance normalized to the normal state (taken as a resistance at $V \simeq 30$ mV) for 3 different contacts with R_0=45, 43, and 111 Ω (curves 1-3, respectively). Main gap $dV/dI-$minima are at about 2.1, 2.6, and 4.86 mV, correspondingly. The larger gap for curve 1 equals 7.0 meV. Curves 2,3 are shifted vertically for clarity.
(b) Raw data of the second harmonic signal V_2 with modulation voltages V_1 =3.31, 2.78, and 2.5 mV, respectively. The numbers of curves are the same as in (a). $T = 4.2$ K, $H = 0$. Curve 1 are shifted vertically for clarity. Their center of symmetry has (0,0) coordinates.

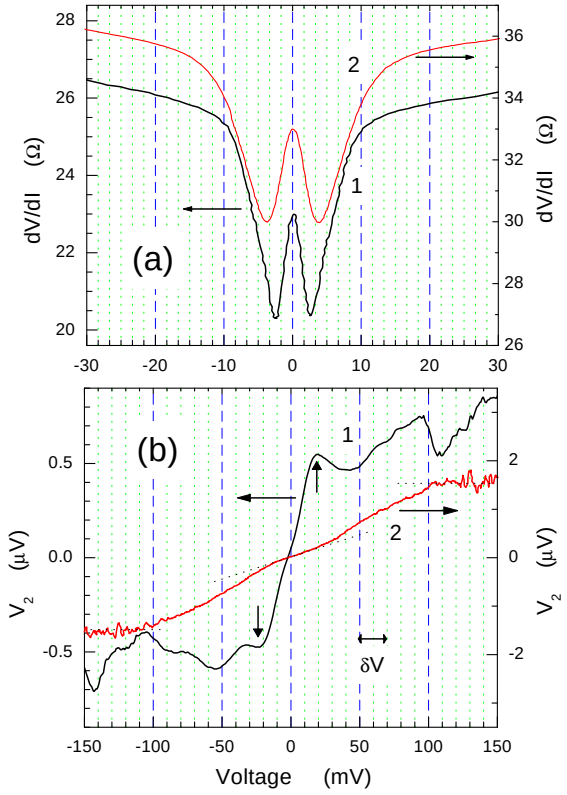

FIG. 3: (a) Differential resistances for MgB_2-Cu point contacts, whose normal state spectra are presented in panel b. $\Delta^{(1)} = 2.55$ meV, $\Delta^{(2)} = 3.69$ meV. T=4.2 K, H=0. (b) Second harmonic signals in the normal state. $V_1 = 2.2$ mV, $T = 41$ K. Note the different Y-scales for curves 1 and 2, which means that the generation of phonons in the latter case is more intensive. For spectrum No.1 the vertical arrows mark the low frequency bumps at about 20 meV. The dotted tangent straight lines point to the phonon features on curve No.2. The horizontal bar with double arrows stands for thermal smearing, determining the spectral resolution δV.

phenomena in the superconducting state. These phenomena are mostly due to destruction of superconductivity in the vicinity of the contact, and lead to depression of the excess current [24]. It has already been noted, that the positions of these nonlinearities are strongly influenced by the field and temperature, and should therefore be disregarded.

As to the spectacular electron-phonon spectrum, presented in our preliminary report (see Fig.3,4 in Ref.[19]), it is presumably a rare example of a direct contribution from the inelastic spectrum of the 2D-band. The magnetic field of 4 T suppresses almost completely the induced phonon features from the 3D-band (with exception of low energy peak). Thus, the proposed tentative consideration would bring our previous observations in line with to what is consistently described here.

The phonon spectra of a contact with a small value of energy gaps are characterized by the presence of low frequency phonon peaks. The small peak at energy of about 25 meV (Fig.4, curves 1,2) is visible, where a tiny knee exists on the PDOS [26] (see PDOS in Fig.1b). In the normal state (at $T \geq T_c$), these low frequency peaks transform into the S-shape structure in $d^2V/dI^2(V)$-spectra (curve 6), corresponding to the wide minimum of $dV/dI(V)$ near zero bias. This low frequency structure is hardly due to the remnants of superconducting quasigap at $T > T_c$, since it is absent in junction No.2, whose characteristic is shown in Fig.3. Rather, it could

be thought of as strong interaction in the 3D-band with very low-frequency excitations, whose origin is not clear yet. On increasing the temperature, the low frequency peak broadens further like common spectral features do in the normal state.

Since most of the current through the point contact is carried by the 3D band with weak EPI, the phonon singularity in the superconducting state is induced mainly by interband scattering from the 2D band with strong EPI. The degree of this induction depends on the interband coupling. As was noted above, in the clean limit the interband coupling in MgB_2 is low [5]. That was the reason for applying the McMillan-proximity-effect model in order to fit the gap structure in $dI/dV(V)$ characteristic in Ref. [7]. This model leads to the small-intensity phonon structure. The elastic scattering, which is certainly high in thin film and may be even stronger by point contact fabrication process, enhances the interband, as well as the intraband coupling. Following Arnold [27], and assuming the extension of the proximity effect theory in coordinate space to the two-band model (i.e. "proximity" effect in k-space), we use the corresponding expression for the interband coupling, induced by elastic scattering in SN sandwiches. In our case, by analogy, the elastic scattering leads to the expression

$$\Delta_1(E) = \frac{Z_1^p \Delta_1^p + i(\hbar/2\tau)\Delta_2(E)N_2(E)}{Z_1^p(E) + i(\hbar/2\tau)N_2(E)}, \qquad (3)$$

which, like the McMillan expression for $\hbar/2\tau = \Gamma_N$ (not shown), derives to $\Delta_1(E) \simeq \Delta_2(E)$, in other words, to the large induced phonon structure in the 3D-band. Here Z_1^p is the renormalization function in the 3D-band, $N_2(E)$ is the electron DOS in the 2D-band, τ is the elastic scattering time, and Γ_N is the interband scattering rate in the McMillan model. Thus, as the interband scattering increases, the intensity of phonon singularity moves to the higher energy, characteristic of the 2D-band. This "internal proximity effect" explains also the small variation in the position (of the order of superconducting energy gap) of phonon peaks with various elastic scattering rates produced by contact fabrication.

The influence of magnetic field on the point-contact spectra is shown in Fig.4 (compare curves 1 and 2). It is evident that the field can smear out the intensity of high energy peaks, which are induced in the 3D-band by EPI of the 2D-band. The disappearance of phonon peaks at rising field and temperature proves that they do not belong to the inelastic backscattering processes, which should have the same intensity both in the superconducting and in normal states. It seems more plausible that the high energy phonon peaks are due to the elastic contribution in the excess current (2) induced by EPI from the 2D band, as was already stated above.

Unfortunately, we cannot estimate the strength of EPI by inelastic PC spectroscopy [22], since we are not able

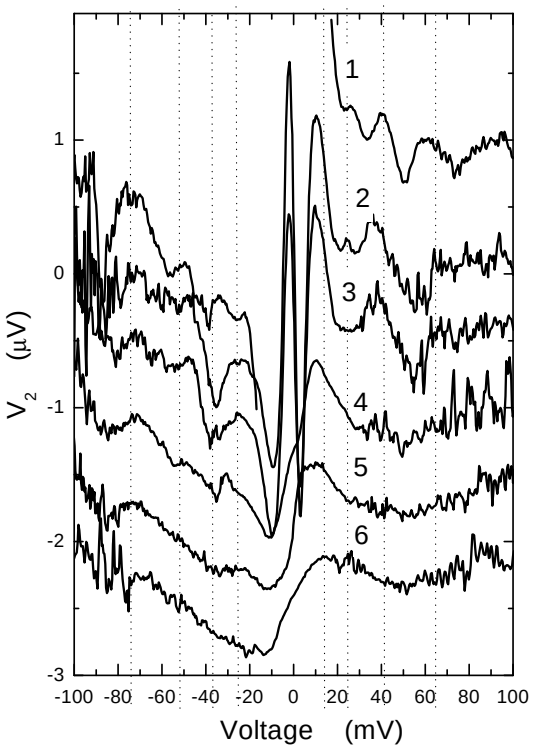

FIG. 4: Second harmonic dependences on field and temperature. The temperature and magnetic field are equal to: 4.2 K, 0 T; 4.2 K, 4 T; 10 K, 4 T; 20 K, 4 T; 30 K, 4 T; 40 K, 0 T, for curves 1-6, respectively. The modulation voltage V_1 is 2.2 mV. Δ=2.7 meV. The vertical dotted lines mark the phonon singularity on the voltage axis. Curves are shifted vertically for clarity, their center of symmetry corresponding to (0,0) coordinates.

to destroy the superconductivity completely by magnetic field at low enough temperature. The latter is necessary to get good resolution. For thin films this experiment will hardly promise encouraging results, since the elastic mean free path is strongly reduced, and the intensity of inelastic backscattering processes is therefore diminished by the factor l/d. Note, that for the superconducting self-energy effects the short elastic mean free path does not suppress essentially the phonon structure [24]. On the contrary, for the two-band model elastic scattering even enhances the phonon structure due to the "intrinsic proximity effect" described above.

Conclusions

We summarize our observation as follows. The reproducible phonon peaks are seen in the superconducting state on $d^2V/dI^2(V)$, and disappear in the normal state, which proves that they are due to the energy dependence of superconducting order parameter. The superconductivity is presumably due to the 2D-band EPI, which in-

duces the $\Delta(E)$ structure in the 3D band. At a small value of the superconducting gap the phonon structure is weak, and its intensity begins to increase with growing Δ. The robustness against the magnetic field also grows notably with increasing Δ.

In the normal state the intensity of the inelastic spectrum also correlates with the value of superconducting gap. The tendency is observed that the high energy phonon peaks become more prominent for a larger gap. For a smaller gap, the low-frequency bump appears in the spectra. It might be due to EPI with some unknown low-frequency excitation [28], but the further work is needed to be sure that it is not caused by phonon peaks of the normal-metal counter electrode (Cu, Ag).

The final goal of PC spectroscopy is to use sufficiently clean material at low temperatures in high enough magnetic field, in order to suppress superconductivity and estimate quantitatively the strength of EPI. The PC experiment, including single crystal technology development, should go in parallel with theoretical calculation, taking into account the specific transport form-factor [22].

Acknowledgements

The work in Ukraine was supported by the State Foundation of Fundamental Research, Grant F7/528-2001.

IKY is grateful to Forschungzentrum Karlsruhe for hospitality, and thanks Dr. Renker for MgB_2 phonon spectrum from Ref.[26].

The work at Postech was supported by the Ministry of Science and Technology of Korea through the Creative Research Initiative Program.

[1] J. Nagamatsu *et al.,* Nature (London) **410**, 63 (2001)
[2] D.M. Buzea and T. Yamashita, Supercond. Sci. Technol. **14**, R115 (2001)
[3] S.V. Shulga *et al.,* cond-mat/0103154
[4] J. Kortus *et al.,* Phys. Rev. Lett **86**, 4656 (2001)
[5] A.Y. Liu, I.I. Mazin, and J. Kortus, Phys. Rev. Lett. **87,** 087005 (2001)
[6] T. Yildirim *et al.,* Phys. Rev. Lett, **87**, 037001 (2001)
[7] H. Schmidt *et al.,* Phys. Rev. Lett. **88**, 127002 (2002)
[8] W.L. McMillan, Phys. Rev. **175**, 537 (1968)
[9] E.L. Wolf, *Principles of Electron Tunneling Spectroscopy,* Oxford, 1985
[10] H. Suhl, B.T. Matthias, and L.R. Walker, Phys. Rev. Lett. **3**, 552 (1959)
[11] C.C. Sung and V.K. Wong, J. Phys. Chem. Solids **28**, 1933 (1967)
[12] V.P. Galaiko, Fiz. Nizk. Temp. **13**, 1102 (1987) [Sov. J. Low Temp. Phys. **13**, No.10 (1987)]
[13] F. Laube, G. Goll, J. Hagel, H. v. Löhneysen, D. Ernst, T. Wolf, Europhys. Lett. **56**, 296 (2001)
[14] M. Iavarone *et al.*, cond-mat/0203329
[15] A. Brinkman *et al.*, Phys. Rev. **B65**, 180517 (2002)
[16] H.J. Choi *et al.,* cond-mat/0111182 and cond-mat/0111183
[17] K.-P. Bohnen, R. Heid, and B. Renker, Phys. Rev. Lett. **86**, 5771 (2001)
[18] Yu.G. Naidyuk, I.K. Yanson *et al.*, JETP Letter **75**, 238-241 (2002)
[19] N.L. Bobrov *et al.,* cond-mat/0110006, to be published in book *"New Trends in Superconductivity"* , eds. J.F. Annett and S. Kruchinin, Kluwer Academic Publishers, Dodrecht, 2002
[20] A.I. D'yachenko *et al.*, cond-mat/0201200
[21] W. N. Kang, Hyeong-Jin Kim, Eun-Mi Choi, C. U. Jung, Sung-Ik Lee, Science **292**, 1521 (2001); W.N. Kang, H.-J. Kim, E.-M. Choi *et al.*, Phys. Rev. Lett. **87**, 087002 (2001)
[22] I.O. Kulik, A.N. Omelyanchouk, and R.I. Shekhter, Sov. J. Low Temp. Phys. **3,** 840 (1977)
[23] I.O. Kulik and I.K. Yanson, Sov. J. Low Temp. Phys. **4**, 596 (1978)
[24] I.K. Yanson, cond-mat/0008116; in book I.O. Kulik and R.Ellialtioglu (eds.)*, Quantum Mesoscopic Phenomena and Mesoscopic Devices in Microelectronic,* p. 61-77, (2000), Kluwer Academic Publishers.
[25] A.N. Omel'yanchuk, S.I. Beloborod'ko and I.O. Kulik, Sov. J. Low Temp. Phys. **14**, 630 (1988)
[26] B. Renker *et al.,* Phys. Rev. Lett **88**, 067001 (2002)
[27] G.B. Arnold, Phys. Rev. B**23**, 1171 (1981)
[28] D. Lampakis, cond-mat/0105447